

1

Technical Report  
900

DTIC FILE COPY

# Geolocation of Frequency-Hopping Transmitters via Satellite

AD-A230 373

DTIC  
ELECTE  
DEC 31 1990  
S D & D

A. Sonnenschein  
W.K. Hutchinson

6 November 1990

**Lincoln Laboratory**

MASSACHUSETTS INSTITUTE OF TECHNOLOGY

LEXINGTON, MASSACHUSETTS



Prepared for the Department of the Air Force  
under Contract F19628-90-C-0002.

Approved for public release; distribution is unlimited.

This report is based on studies performed at Lincoln Laboratory, a center for research operated by Massachusetts Institute of Technology. The work was sponsored by the Department of the Air Force under Contract F19628-90-C-0002.

This report may be reproduced to satisfy needs of U.S. Government agencies.

The ESD Public Affairs Office has reviewed this report, and it is releasable to the National Technical Information Service, where it will be available to the general public, including foreign nationals.

This technical report has been reviewed and is approved for publication.

FOR THE COMMANDER

*Hugh L. Southall*

Hugh L. Southall, Lt. Col., USAF  
Chief, ESD Lincoln Laboratory Project Office

Non-Lincoln Recipients

**PLEASE DO NOT RETURN**

Permission is given to destroy this document  
when it is no longer needed.

**MASSACHUSETTS INSTITUTE OF TECHNOLOGY  
LINCOLN LABORATORY**

**GEOLOCATION OF FREQUENCY-HOPPING TRANSMITTERS  
VIA SATELLITE**

**A. SONNENSCHNEIN  
W.K. HUTCHINSON**  
*Group 64*

**TECHNICAL REPORT 900**

**6 NOVEMBER 1990**

**Approved for public release; distribution is unlimited.**

**LEXINGTON**

**MASSACHUSETTS**

## ABSTRACT

A satellite-communications terminal geolocation is analyzed by satellite interception, whereby a number of spaceborne interceptors transpond the frequency band of interest to a terrestrial location for processing. The general formulas for the interception accuracy are summarized, and a strawman interceptor system is proposed. Interception regions for prototypical terminals and satellites are calculated and the results are presented parametrically as a function of uplink SNR. The optimum angular separation of the interceptor satellites is found, and the effect of nonoptimal separation is discussed. The practical limitations involved in implementing this geolocation system are also discussed.



Accession For	
NTIS CRA&I	<input checked="" type="checkbox"/>
DTIC TAB	<input type="checkbox"/>
Unannounced	<input type="checkbox"/>
Justification	
By	
Distribution /	
Availability Codes	
Dist	Avail and/or Special
A-1	

## ACKNOWLEDGMENTS

The authors wish to thank W.C. Cummings, D.R. McElroy, and J.E. Kaufmann for useful discussions.

## TABLE OF CONTENTS

Abstract	iii
Acknowledgments	v
List of Illustrations	ix
List of Tables	xi
1. INTRODUCTION	1
2. CRAMÉR RAO BOUNDS ON THE GEOLOCATION ERROR	3
3. STRAWMAN INTERCEPTOR SYSTEM	7
4. LINK BUDGET	9
5. OPTIMUM ANGULAR SEPARATION OF INTERCEPTORS	11
5.1 Optimum Angle for a $J_1(x)/x$ Transmitter Antenna Pattern	11
5.2 Optimum Angle for a $J_3(x)/x^3$ Transmitter Antenna Pattern	14
5.3 Optimum Interceptor Separation	14
6. GEOLOCATION OF TERMINALS: IDEAL PERFORMANCE	19
7. OBSERVATIONS	21
7.1 Interceptor G/T	21
7.2 Restricting the Search Window	21
8. CONCLUSION	23
REFERENCES	25

## LIST OF ILLUSTRATIONS

Figure No.		Page
1	Components of geolocation system.	1
2	Strawman interceptor system.	8
3	Relative geolocation SNR as a function of angular separation; $J_1(x)/x$ antenna pattern; $\square$ configuration.	12
4	Relative gain from various transmitter apertures.	15
5	Relative geolocation SNR for various transmitter apertures.	16
6	$1-\sigma$ geolocation error.	19

## LIST OF TABLES

Table No.		Page
1	Prototypical Terminal Characteristics	9
2	Uplink Signal-to-Noise Ratios	10

# 1. INTRODUCTION

This report analyzes an emitter-location technique that involves spaceborne interception of ground-to-satellite communication links. In this scheme a number of interceptor satellites transpond the frequency band of interest to a terrestrial location for processing, as shown in Figure 1. The basic technique can be used on a variety of signal types: fixed-frequency, frequency-hopped, pseudo-noise, etc. However, the focus throughout this report is the theoretical feasibility of geolocating terminals that are hopping in frequency. The technique is applicable at any frequency, but, to simplify the formulation, we assume that the ground terminals have narrow antenna beamwidths and they operate in the higher satellite communication frequency bands.

158125-1

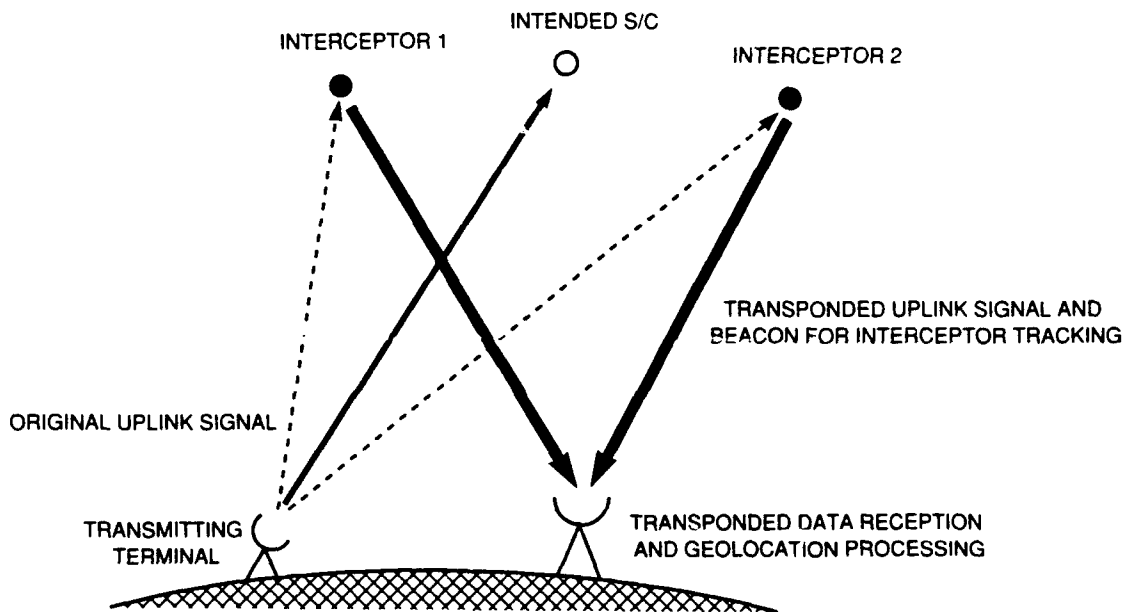


Figure 1. Components of geolocation system.

The time of arrival of a signal having a known structure can be estimated by correlating the incoming signal with a replica and finding the peak of the correlation function. In the case of a signal having an unknown structure that arrives at two separate receivers, the differential time of

arrival (DTOA) can be similarly found by forming the correlation function<sup>1</sup> of the two receiver outputs. Uncertainty in frequency as well as in time leads to the generalization of the correlation function known as the complex ambiguity function [1]

$$A(\tau, f) = \int_0^T s_1(t) s_2^*(t + \tau) e^{-j2\pi f t} dt \quad , \quad (1)$$

where  $s_1$  and  $s_2$  are the complex envelopes of two signals that have some common features.  $|A(\tau, f)|$  achieves its peak for values of  $\tau$  and  $f$  that are the complements of the relative time and frequency offsets of the two signals.

Given the complex-ambiguity-function data, the use of a reasonable peak-location algorithm will yield estimates of the signals' DTOA and differential frequency of arrival (also known as differential Doppler, or DD for short). For a reasonably high signal-to-noise ratio (SNR), the algorithm will come close to achieving the Cramér-Rao bounds for DTOA and DD estimation [1]. Multiple hyperboloids that correspond to constant values of DTOA or DD intersect the earth, each forming a line-of-position (LOP). The intersection or near-intersection of multiple LOPs yields the geolocation estimate, the accuracy of which can be derived in terms of the accuracies of the DTOA and the DD estimates [2].

A summary of known formulas for the accuracy of the DTOA-based estimates and the resulting geolocation are provided in the following section. Emphasis is placed on the simplifications that ensue when the formulas are applied to ideal satellite interception of a relatively narrow-beam transmitted signal.<sup>2</sup>

---

<sup>1</sup>Frequently, this is also called the cross-correlation function.

<sup>2</sup>Although similar results for DD-based geolocation can be readily developed, they will not be explicitly considered in this report.

## 2. CRAMÉR RAO BOUNDS ON THE GEOLOCATION ERROR

Let  $B_s$  be the signal bandwidth,  $B$  the noise bandwidth, and  $T$  the duration of the waveform that is processed. Furthermore,  $\gamma_{out}$  is defined to be the effective SNR, i.e.,  $P_s/(N_0B)$ , at the *output* of the (complex) cross-correlator. The cross-correlator's output SNR can be expressed in terms of the input SNRs as

$$\gamma_{out} = BT \frac{\gamma_1 \gamma_2}{1 + \gamma_1 + \gamma_2} \quad (2)$$

where  $\gamma_1$  and  $\gamma_2$  are the SNRs at the inputs of the two receivers. Assuming the input SNRs are equal ( $\gamma_1 = \gamma_2 \triangleq \gamma_{in}$ ), Equation (2) takes on the standard form of the cross-correlator input/output SNR characteristic

$$\gamma_{out} = BT \frac{\gamma_{in}^2}{1 + 2\gamma_{in}} \quad (3)$$

Making the substitution  $\frac{E}{N_0} = BT\gamma$ , Equation (3) can be rewritten as

$$\left(\frac{E}{N_0}\right)_{out} = \frac{BT \left(\frac{E}{N_0}\right)_{in}^2}{BT + 2 \left(\frac{E}{N_0}\right)_{in}} \quad (4)$$

This equation indicates the input/output SNR relationship is linear at high SNR and square-law at low SNR, with a crossover at about -2 dB.

Hereafter, it will be assumed that  $\frac{E}{N_0}$  refers to the identical SNRs at the inputs of the receivers, and that  $B = 1/T = B_s =$  the hopping frequency. The latter assumption, which is valid when there is but one chip per uplink hop,<sup>3</sup> implies that  $\gamma_{out} = (E/N_0)_{out}|_{BT=1}$ .

The  $1-\sigma$  error for the DTOA estimate is [1]

$$\sigma_{DTOA} = \frac{\sqrt{3}}{\pi B_s} \frac{1}{\sqrt{2\gamma_{out}}}$$

---

<sup>3</sup>An example of a one-chip-per-hop situation is frequency-hopped M-ary FSK modulation, where each hop consists of a single FSK tone.

$$= \frac{\sqrt{3}}{\pi B_s} \sqrt{\frac{1 + 2(E/N_0)}{2(E/N_0)^2}} \quad (5)$$

This result holds for a spectrum that is rectangular over the band  $B_s$ .

Since the line of constant DTOA corresponds to an LOP on the earth, the variance of the DTOA estimate can be directly related to the variance of the location estimate (along each axis) by the formula [2]

$$\sigma_1 = \left[ \frac{c^2 \sigma_{DTOA}^2 + 2\sigma_p^2}{4 \sin^2(\theta/2) - (\cos \phi_2 - \cos \phi_1)^2} \right]^{1/2}, \quad (6)$$

where  $c$  is the speed of light,  $\sigma_p$  is the  $1-\sigma$  error in each of the interceptor coordinates,  $\phi_i$  is the pointing angle from the transmitter to receiver  $i$ , and  $\theta \triangleq |\phi_2 - \phi_1|$  is the angle separating the two receivers when viewed from the transmitter.

For the case of very accurate measurements of the receivers' positions,<sup>4</sup> and the small subtending angle  $\theta$  that is of interest at high frequencies, Equation (6) can be simplified by using  $\sigma_p \approx 0$ ,  $\cos \phi_1 \approx \cos \phi_2$ , and  $\sin \theta/2 \approx \theta/2$ :

$$\sigma_1 \approx \frac{c \sigma_{DTOA}}{\theta} \quad (7)$$

Assume that the separation angle  $\theta$  is equal to the half-power-beamwidth (HPBW) of the transmitting antenna.<sup>5</sup> The HPBW is given by the usual formula

$$HPBW = 1.22 \frac{c}{fD} \text{ radians}, \quad (8)$$

where  $f$  is the signal's frequency and  $D$  is the diameter of the circular aperture antenna. Substituting this equation, along with (5), into (7), and assuming two similar, independent and orthogonal<sup>6</sup>

<sup>4</sup>This would be essentially true if skin-tracking radar was used.

<sup>5</sup>The variation of geolocation performance with separation angle is considered in Section 5.

<sup>6</sup>If the LOPs (labeled  $A$  and  $B$ , say) are not orthogonal, but rather have an angle of intersection  $\psi$ , then the resulting  $1-\sigma$  error is  $\sigma = \sqrt{\sigma_A^2 + \sigma_B^2} / \sqrt{\sin \psi}$ .

LOPs due to two DTOA estimates, the final  $1-\sigma$  geolocation error is

$$\begin{aligned}\sigma = \sqrt{2}\sigma_1 &= 2.3 \times 10^5 \frac{1}{B_s \cdot \text{HPBW}} \sqrt{\frac{1 + 2(E/N_0)}{2(E/N_0)^2}} \text{ km} \\ &= 6.4 \times 10^{-4} \frac{fD}{B_s} \sqrt{\frac{1 + 2(E/N_0)}{2(E/N_0)^2}} \text{ km} \quad ,\end{aligned}\tag{9}$$

where  $D$  is given in meters, and  $f$  and  $B_s$  are given in hertz. For the sake of generality, the form given in (9) will be used henceforth.

Similar equations can be derived for the geolocation error based on DD estimates. In either case, whether DTOA- or DD-based data is used, averaging over  $N$  independent sets of measurements decreases the location error by a factor of  $1/\sqrt{N}$ .

### 3. STRAWMAN INTERCEPTOR SYSTEM

To geolocate a transmitting terminal, at least two independent LOPs have to be obtained. This can be done simultaneously with only two interceptors (provided both DTOA and DD estimates are used) or with three interceptors (if only one type of estimate is used). Using successive gatherings of the DTOA estimate, it is possible to unambiguously locate the terminal with only two interceptors, provided they are moving with respect to the terminal. Indeed, the latter method can be applied with only one interceptor if the ephemerides of both the intended satellite and the interceptor are accurately known, as are the epoch timing boundaries of the system. This report, however, concentrates on the situation of multiple interceptors providing DTOA estimates. No assumptions of accurate satellite ephemerides or knowledge of epoch timing are made, though the ephemerides of the interceptors are assumed to be very accurately known.

Figure 2 illustrates the two specific interceptor configurations. The first configuration consists of four interceptors placed at the vertices of a box (approximately), centered on the intended satellite. Similarly, in the second configuration, three interceptors form an equilateral triangle about the satellite. In both the box and the triangle configurations, which will be symbolized by  $\square$  and  $\triangle$ , respectively, the pair-wise angular spacing of the interceptors is denoted by  $\theta$ . The distance between each interceptor and the satellite is  $\theta/2$  for the  $\square$  scenario and  $\theta/\sqrt{3}$  for the  $\triangle$  scenario.

For each of these configurations there is an optimal value of  $\theta$  that allows the most accurate estimation. As shown in Section 5, a value of  $\theta = 1$  HPBW is very nearly optimal for both the  $\square$  and the  $\triangle$  scenarios. Furthermore, calculations indicate that geolocation based on the  $\triangle$  configuration is 13.5 percent less accurate than one based on the  $\square$  configuration, corresponding to an effective loss in geolocation SNR of 1.1 dB.

The strawman interceptor system will be the  $\square$  configuration with 1 HPBW spacing between interceptors. This choice maximizes the estimation accuracy, though it clearly requires more in-orbit assets. Using the formulas and graphs of Section 5, it is a straightforward matter to extend the results from that of the strawman system to a  $\square$  or  $\triangle$  configuration of arbitrary interceptor spacing.

Assuming the cross-correlation signal peak can be detected in all cases, source location accuracy can be enhanced by correlating longer spans of data and/or averaging successive DTOA estimates. Frequency hopping by the source terminal seriously impedes the geolocation procedure *only* if the resulting SNRs of the hops seen at the interceptors are too low to allow reliable detection of the peak of the ambiguity function. In such a case, it would be necessary to collect and sort multiple hops from all the active sources in the monitored area, a problematical task. On the other hand, if the SNRs are high enough, a DTOA estimate can be derived from each hop's data and then the numerous, albeit crude, one-hop estimates can be averaged to yield the desired accuracy.

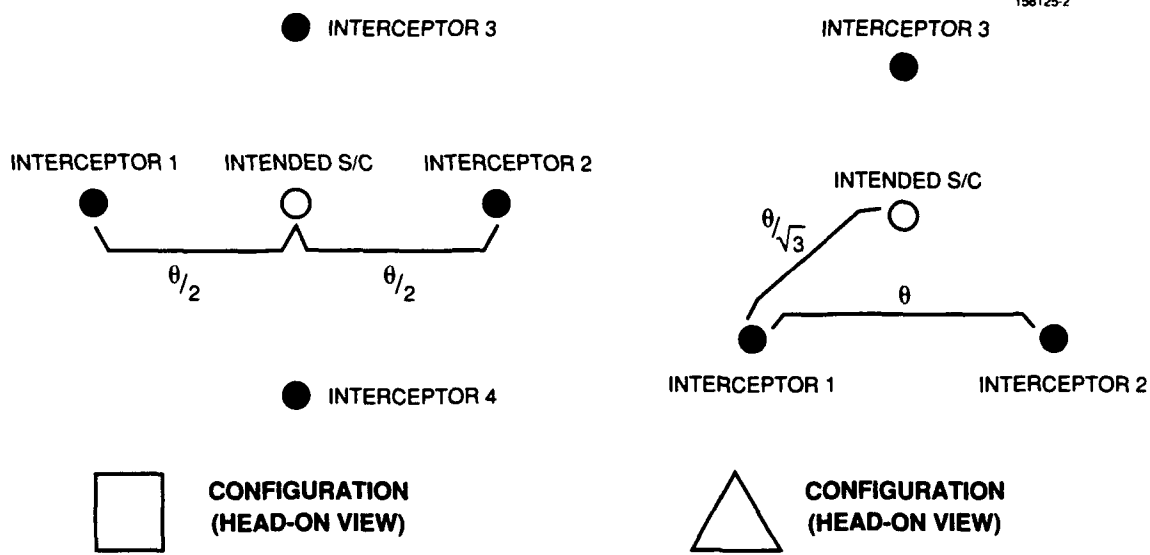


Figure 2. Strawman interceptor system.

#### 4. LINK BUDGET

In the strawman interceptor system, the geolocation accuracy formula given in Equation (9) is a function of three parameters: the user signal bandwidth  $B_s$ , the input SNR, and the transmitting terminal's uplink HPBW. The latter two parameters are quantified below for various terminals.

The received power-to-noise ratio at a satellite from a terrestrial terminal is

$$(P_r/N_0)_{\text{satellite}} = (EIRP)_{\text{terminal}} - 10 \log(kT) - L_{\text{misc}} - 20 \log R - 10 \log(4\pi) + 10 \log A \quad \text{dB-Hz} \quad (10)$$

where  $k$  is Boltzmann's constant (-228.6 dBW/K-Hz);  $T$  is the satellite system temperature;  $L_{\text{misc}}$  is a term into which all the miscellaneous losses are folded;  $R$  is the path length; and  $A$  is the effective satellite antenna aperture area. Assuming  $T = 1000$  K,  $L_{\text{misc}} = 2$  dB,  $R = 40,000$  km, and a couple of reasonably-sized satellite apertures, (10) becomes

$$(P_r/N_0)_{\text{satellite}} = \begin{cases} (EIRP)_{\text{terminal}} + 20 \quad \text{dB-Hz, for } A = 430\text{cm}^2 \\ (EIRP)_{\text{terminal}} + 5 \quad \text{dB-Hz, for } A = 15\text{cm}^2 \end{cases} \quad (11)$$

The apertures and system temperatures, which are assumed to be the same for both the intended satellite and the interceptor satellites, should be easily attainable.

Table 1 enumerates the EIRPs and the uplink half-power-beamwidths of a couple of prototypical terminals.

**TABLE 1**  
**Prototypical Terminal Characteristics**

Terminal Type	Terminal EIRP (dBW)	Uplink HPBW (radians)
Type A	60	0.014
Type B	45	0.062

Assuming the hopping rate is 1000 hops-per-second, Table 2 lists the received SNR per hop as a function of the terminal type and the effective satellite aperture. Note that the full-power

SNR is sufficient to allow reliable peak-detection based on a single intercepted hop's worth of data, mostly by a substantial margin. Reduction of this margin would entail the use of lower-power transmissions, which could necessitate the terminal's use of lower data rates.

**TABLE 2**  
**Uplink Signal-to-Noise Ratios**

Effective Satellite Aperture	Uplink $E/N_0$ (dB)	
	Type A Terminal	Type B Terminal
430 cm <sup>2</sup>	50	35
5 cm <sup>2</sup>	35	20

## 5. OPTIMUM ANGULAR SEPARATION OF INTERCEPTORS

Until now, we have assumed the separation angle  $\theta$  to be equal to the transmitting antenna's HPBW. This section investigates the effect on the geolocation error  $\sigma$  using a different angle  $\theta$ .

The angle  $\theta$  enters the geolocation calculations directly, as an indicator of the baseline of an interceptor pair, and indirectly, through the reduction in the received SNR caused by the misdirection of the transmitter's antenna gain pattern. These are opposing effects in that an increased  $\theta$  tends to both enhance the estimator accuracy (by increasing the baseline) and degrade it (by reducing the received SNR and making it more difficult to detect the peak of the ambiguity function). The conglomerate effect is quantified below.

### 5.1 Optimum Angle for a $J_1(x)/x$ Transmitter Antenna Pattern

#### 5.1.1 Box ( $\square$ ) Interceptor Configuration

First, consider the ideal power gain pattern of a uniformly-illuminated circular aperture:

$$G(\phi) = \left[ 2 \frac{J_1(3.23\phi)}{(3.23\phi)} \right]^2, \quad (12)$$

where  $\phi$  is the angular offset in HPBW, and the peak gain has been normalized to unity. As demonstrated by the gains of the first five sidelobes ( $-17.6$ ,  $-23.8$ ,  $-28.0$ ,  $-31.1$ , and  $-33.7$  dB, respectively), the gain falls off fairly rapidly. Intuitively, it may seem that this quick decline, coupled with the narrow beamwidths seen at high frequencies, forces the interceptors to be near the peak of the main lobe if they are to be at all effective. This is indeed the case if the signal is undetectable when seen through a sidelobe, thereby forcing the main lobe to be used. However, if the signal level is sufficiently high to allow reasonable detection through a sidelobe, geolocation using that sidelobe's signal is possible, though it is certainly not as efficient as using the main lobe's signal.

As is evident from Equation (9), the geolocation variance  $\sigma^2$  is proportional to  $[\theta^2 SNR]^{-1}$ , where  $SNR$  is an implicit function of  $\theta$  by way of the transmitting terminal's gain pattern. Denoting the (power) gain pattern by  $G(\cdot)$ , the following proportionality relation can be written:

$$\sigma^2 \propto \frac{1}{\theta^2 SNR} \propto \frac{1}{\theta^2 G(\theta/2)}. \quad (13)$$

When the interceptor spacing  $\theta$  is changed from, say,  $\theta_{old}$  to  $\theta$ , the relative change in the SNR needed for an equivalent geolocation variance is

$$\Delta SNR \triangleq \frac{\theta^2 G(\theta/2)}{\theta_{old}^2 G(\theta_{old}/2)} \quad (14)$$

Using  $\theta_{old} = 1$  HPBW as the reference point, Equation (14) becomes

$$\Delta SNR = 2 \theta^2 G(\theta/2) \quad , \quad (15)$$

where  $\theta$  is given in units of HPBW.

Figure 3 plots <sup>7</sup> Equation (15), as well as  $G(\theta/2)$ , as a function of  $\theta$ .

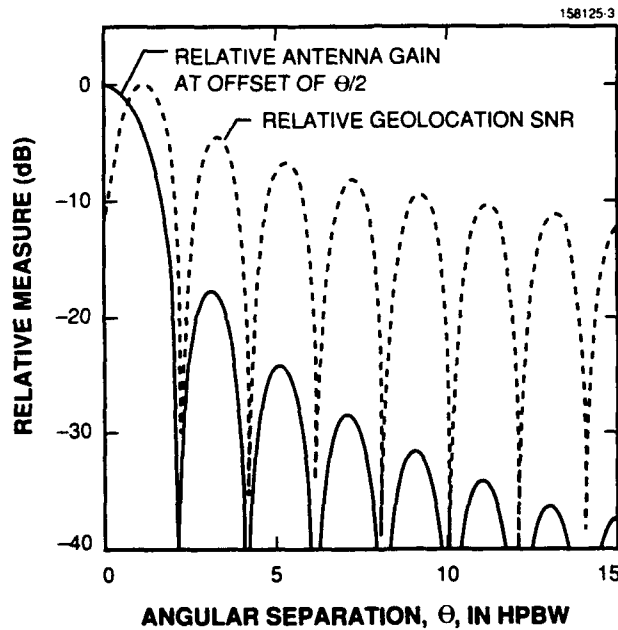


Figure 3. Relative geolocation SNR as a function of angular separation;  $J_1(x)/x$  antenna pattern; □ configuration.

<sup>7</sup>Unless otherwise stated, a  $J_1(x)/x$  antenna pattern is assumed.

This figure shows the geolocation efficiency of using various values of  $\theta$  relative to that of using  $\theta = 1$  HPBW, provided that detection is possible at an angular offset of  $\theta/2$  from the peak of the transmitter's antenna pattern (which is pointing at the intended satellite). The latter condition is necessary since an increased interceptor baseline is useless if the signal is undetectable.

The peak geolocation efficiency occurs at  $\theta \approx 1$  HPBW, while the peaks of subsequent efficiency lobes occur at about the locations that correspond to the sidelobes of the gain pattern. That is, the first four efficiency peaks (after that of the main lobe) are at  $\theta = 3.2, 5.2, 7.2,$  and  $9.2$  HPBW respectively, with corresponding relative SNR degradations of  $-4.5, -6.5, -7.8,$  and  $-8.8$  dB. If a sidelobe's signal is detectable, then that signal can also be used for geolocation, with much of the apparent loss in SNR (relative to the optimum of  $\theta = 1$  HPBW) being compensated by the increase in the baseline.

### 5.1.2 Triangle ( $\Delta$ ) Interceptor Configuration

The previous calculations have assumed a  $\square$  interceptor configuration, as defined in Section 3. Similar results can be derived for the  $\Delta$  configuration, using a variation of Equation (15) that takes into account the change of the interceptor-to-satellite spacing from  $\theta/2$  to  $\theta/\sqrt{3}$ :

$$\Delta SNR = 2.57 \theta^2 G(\theta/\sqrt{3}) \quad (16)$$

Evaluation of this equation indicates the optimal efficiency and the associated  $\theta$  ( $\approx 1$  HPBW) to be about the same as for the  $\square$  configuration. For the  $\Delta$  array, this implies the interceptor SNR is  $G(1/\sqrt{3}) = -4.1$  dB from the peak seen at the intended satellite, rather than  $-3$  dB from the peak for the  $\square$  array. Of course, the spacings between and the values of the subsequent peaks are different from the  $\square$  case.

Comparing the optimal geolocation performance of the  $\Delta$  interceptor array with that of the  $\square$  array, with  $\theta_{opt} = 1$  HPBW in either case,

$$\frac{\sigma_{\Delta,opt}}{\sigma_{\square,opt}} = \frac{\sqrt{G(1/2)}}{\sqrt{G(1/\sqrt{3})}} = 1.135 \quad (17)$$

This 13.5 percent degradation in geolocation accuracy corresponds to an equivalent loss in SNR of 1.1 dB, so that  $\sim 29$  percent more samples need to be averaged in the  $\Delta$  array to equal the performance of the  $\square$  array.

## 5.2 Optimum Angle for a $J_3(x)/x^3$ Transmitter Antenna Pattern

It was demonstrated in Section 5.1 that, for a transmitter having a typical antenna gain pattern [such as the ideal  $J_1(x)/x$ ], geolocation using the transmitter's sidelobes is feasible, provided the SNR at each interceptor is high enough to allow detection of the signal.

When the sidelobes of the transmitting antenna gain pattern are reduced, e.g., by modifying the feed, the resulting decrease in detectability may be sufficient to restrict all practical interceptor separation angles to be in the region of the main lobe. In such a case, realistic limitations on the minimum interceptor-to-satellite orbital distance would allow geolocation of only those terminals that have small antennas. The terminals having larger antennas (and smaller HPBWs) would require unrealistically small interceptor-to-S/C orbital distances.

As an example, parabolic-squared tapering [3] of the antenna feed produces a low-sidelobe gain pattern that has the form  $J_3(x)/x^3$ . The first sidelobe of the  $J_3(x)/x^3$  pattern is more than 30 dB down from the peak, which is about the same level as for the fourth sidelobe of the  $J_1(x)/x$  pattern. Sidelobe geolocation that is feasible by a margin of less than 12 dB for a  $J_1(x)/x$  pattern is not feasible for the case of a  $J_3(x)/x^3$  pattern. Mainlobe geolocation is similar for both patterns.

As in the  $J_1(x)/x$  case, the relative degradation in the  $J_3(x)/x^3$  geolocation accuracy, due to a change from a  $\square$  configuration to a  $\triangle$  configuration, is about 1 dB, requiring about 26 percent more data for equivalent performance.

## 5.3 Optimum Interceptor Separation

The generic interceptor-separation results of Section 5.1 can be applied to the terminals listed in Section 4. With uniformly-illuminated transmitter apertures, a  $\square$  interceptor configuration, and a transmitter-to-satellite distance of<sup>8</sup>  $R = 40,000$  km, the relative antenna gains of the two terminal types are shown in Figure 4 as a function of the interceptor-to-S/C distance ( $\approx R\theta/2$ ). Figure 5 graphs the relative geolocation SNRs for the two apertures also as a function of the interceptor-to-S/C distance, hereafter referred to as  $\mathcal{D}$ . That is, in comparison with the point  $\mathcal{D}_{\theta=1 \text{ HPBW}}$ , the geolocation accuracy is reduced by an amount equivalent to the drop in SNR depicted in Figure 5.

### 5.3.1 Optimization for Each Terminal

Figure 5 illustrates that the optimum values of  $\mathcal{D}$  (corresponding to a  $\theta$  of 1 HPBW) are 270 km and 1230 km for the Type-A and Type-B apertures, respectively. These are the *individually* optimum values of  $\mathcal{D}$ , assuming no restriction on the minimum distance. The imposition

---

<sup>8</sup>A 20° elevation look angle and geostationary-altitude satellites are assumed.

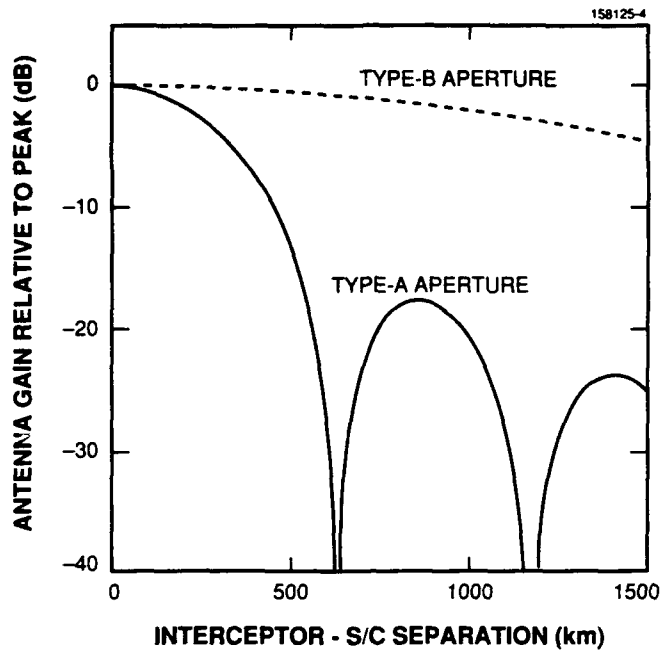


Figure 4. Relative gain from various transmitter apertures.

of a restriction on  $\mathcal{D}$  modifies the corresponding values of  $\mathcal{D}_{opt}$ , as demonstrated by the following examples.

If  $\mathcal{D}$  is restricted to be  $\geq \sim 500$  km,  $\mathcal{D} = \mathcal{D}_{HPBW}$  for the Type-B antenna as before, the Type-A terminal must be detected through its first sidelobe ( $\mathcal{D} = 860$  km). The effective loss in geolocation SNR of the latter terminal is only 4.5 dB, *provided* the ambiguity peak can be detected despite the 14.6 dB reduction in gain relative to the 3-dB point.

In a similar manner, extending the lower limit of  $\mathcal{D}$  to  $\sim 1000$  km forces the Type-A terminal to be received through its second sidelobe. It is essential to keep in mind that the small relative degradations in geolocation SNR illustrated in Figure 5 assume that the peak of the ambiguity function is reliably detectable. The practicality of detecting the peak is determined by the curves of Figure 4 coupled with the EIRPs and link budgets of Section 4.

### 5.3.2 Joint Optimization

In the previous section, the optimum interceptor-S/C distance  $\mathcal{D}$  was considered separately for each source with a given antenna size, and under various limitations on  $\mathcal{D}$ . To detect both source types simultaneously, the jointly optimum distance is equal to the optimum distance of the smaller aperture, provided there is sufficient margin to detect the ambiguity peak on the appropriate

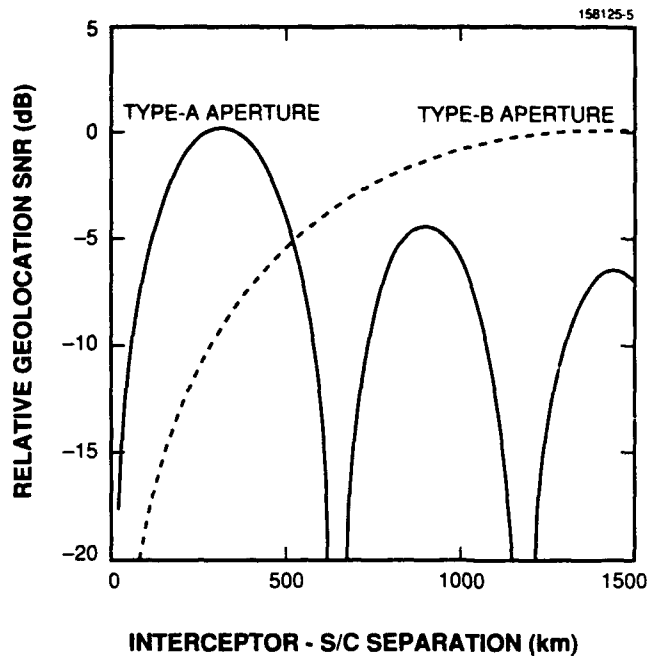


Figure 5. Relative geolocation SNR for various transmitter apertures.

antenna sidelobes. However, insufficient sidelobe margins may force the use of a smaller  $\mathcal{D}$  to allow peak detection, with a concomitant increase in the amount of data required to achieve the desired geolocation accuracy.

Consider the joint geolocation of Type-A and Type-B terminals. Selecting a  $\mathcal{D}$  of 860 km puts the interceptor at the peak of the larger antenna's first sidelobe and well within the main lobe of the smaller antenna. The relative antenna gains are -14.6 dB and +1.6 dB, respectively, and the corresponding relative geolocation SNRs are -4.5 dB and -1.5 dB.<sup>9</sup>

On the other hand, having  $\mathcal{D} = 270$  km lets the interceptor be at  $\mathcal{D}_{HPBW}$  for the Type-A source; this distance places the interceptor near the peak of the Type-B source. The relative gain and geolocation SNR of the Type-A source are both 0 dB, while those for the Type-B source are +2.9 dB and -10.3 dB, respectively. In other words, for the case of the smaller-aperture source the

<sup>9</sup>The gains referred to are the antenna power gains at a given  $\mathcal{D}$  relative to the gains at  $\mathcal{D}_{HPBW}$ , or 3 dB down from the mainlobe peak. Similarly, the geolocation SNRs are presented relative to the optimum values, which occur at  $\mathcal{D} = \mathcal{D}_{HPBW}$ .

relative gain is increased, but the reduced baseline causes a reduction in the relative geolocation accuracy, thereby extending the required data-gathering.

The choice between the above two options for  $\mathcal{D}$  depends upon the uplink margins of the sources, their relative importance, and the limitations, if any, on the maximum assured duration of data. The use of these guidelines is illustrated by the following special case: if the smaller sources are more important, there are no severe time limitations, and the larger sources have uplink margins (to the intended satellite) of at least  $\sim 20$  dB, then the appropriate choice for  $\mathcal{D}$  is<sup>10</sup> 860 km.

---

<sup>10</sup>This value is for geostationary satellites and interceptors with the appropriate angular spacing, viewed from an elevation angle of  $20^\circ$ . The distance decreases with increasing elevation angle, reaching 780 km at  $90^\circ$ .

## 6. GEOLOCATION OF TERMINALS: IDEAL PERFORMANCE

The Cramér-Rao bounds on the geolocation error, detailed in Section 2, will now be used to calculate the geolocation regions for the terminals detailed in Tables 2 and 1. Throughout the following it is assumed that the  $\square$  interceptor configuration is used, with an angular spacing between opposing interceptors of  $\theta = 1$  HPBW. The interceptor-spacecraft distances ( $\mathcal{D}$ ) associated with this optimum angular spacing for Type-A and Type-B aperture sources are at 270 and 1230 km, respectively. The effect of other nonoptimal values of  $\mathcal{D}$  on the results presented below can be calculated using the graphs previously given in Section 5.

For each terminal type and each filter bandwidth ( $B_s$ ), Equation (9) was used to calculate the  $1-\sigma$  geolocation error for DTOA-only measurements as a function of the input SNR at the interceptors' front ends. The geolocation results, presented in Figure 6, are for the reception of a *single hop* having an SNR of  $E/N_0$ . As always, a prerequisite for this geolocation accuracy is the detection of the peak of the ambiguity function.

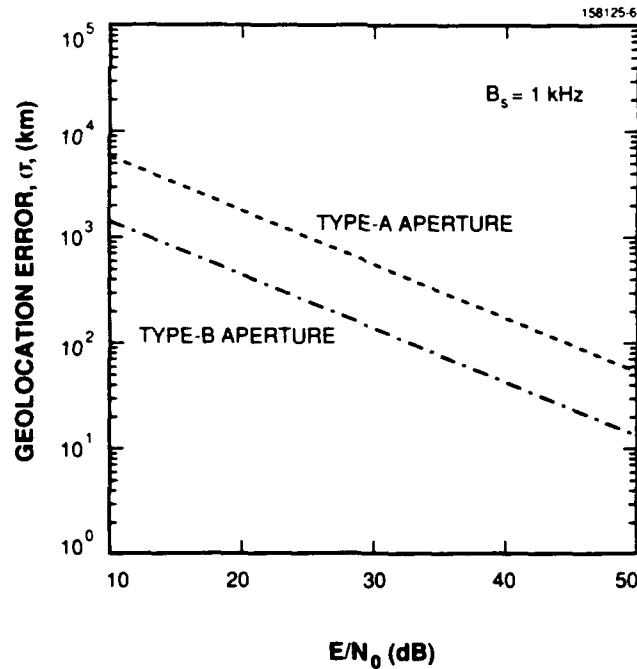


Figure 6.  $1-\sigma$  geolocation error.

When the SNR at the interceptor is greater than about 15 dB, a single hop is sufficient to detect the peak. Often, a 10 dB SNR is used as a rule of thumb to indicate reliable detection based on a single measurement [1]. In a very wide hopping band, however, the number of time-frequency cells that are to be searched for a detection is very large, and the required false-alarm probability *per cell* is extremely small, thereby requiring a higher SNR (such as 15 dB) in order to make a detection decision on the basis of only a single hop. Nevertheless, peak detection is possible at a much lower SNR, but the decision is then made using multiple hop measurements, and the peak estimation is done in a decision-directed manner using the same stored measurements.

## 7. OBSERVATIONS

### 7.1 Interceptor G/T

It was assumed in Section 4 that the receiver antenna apertures of the intended satellite and each interceptor were rather small. However, the type of antenna employed by a practical interceptor could range from a small-aperture earth-coverage horn to a larger-aperture narrow spot beam antenna. If the interceptor's antenna aperture was considerably greater than that of the intended satellite, the intercept region of the terminals transmitting into that beam would be substantially increased.

For example, if a terminal is transmitting both into the intended satellite's earth-coverage beam and into an interceptor's spot beam, the transmitter would be very easily detected and geolocated. The interceptor's considerable detection margin could be used either to geolocate terminals through the sidelobes of their uplink beams or to restrict the search window in the manner indicated in the following section.

An additional benefit to the interceptors using highly directional antennas is the inherent spatial discrimination that they would provide, making it easier to separate the presence of a number of transmitters in the region being monitored.

On the other hand, if the interceptor satellites are using broad uplink beams while the intended satellite has a pencil beam, the signals received by the interceptors will be much weaker, and geolocation will be more difficult.

### 7.2 Restricting the Search Window

In many of the likely scenarios the SNR received by the interceptors will be substantial, i.e., greater than 15 dB, and the number of hops needed for geolocation will not be very large. Therefore, the search procedure can be considerably restricted in any of several dimensions (namely, frequency, space, and time) and still provide very quick geolocation.

First, and probably most importantly, only a portion of the hopping band may be monitored. If the transmitting terminal hops uniformly across the frequency band, enough data can still be collected to form a good geolocation estimate.

Second, in the case of the interceptors having highly directive beams, they can be coordinated to scan across a region. Because for geolocation at moderate-to-high SNR only a few hops are necessary, the periodic coverage of the entire area would be adequate to catch transmissions that last more than a few seconds.

Finally, the processing in the ground station need not be done in real time. The station may take, say, 1 s to process 100 ms worth of data, for a duty cycle of 9 percent. In many cases, this partial temporal coverage will provide adequate geolocation service.

## 8. CONCLUSION

The results of the theoretical calculations detailed in this report indicate that geolocation of frequency-hopping terminals by a network of spaceborne interceptors and an accompanying terrestrial processing station is feasible under the indicated conditions. The optimum angular separation of the interceptor satellites was found to be approximately equal to the uplink HPBW of the transmitting antenna, and the effect of nonoptimal separation was discussed. A system to geolocate several terminal types would require a compromise choice for the interceptor separation because different types of terminals have different uplink HPBWs. The extent of the compromise would depend on the relative value afforded by the interception of the various terminals.

As a final point, it should be noted that considerable effort is involved in forming the geolocation system type detailed in this report. To create such a system it would be necessary to:

- Place, maintain in appropriate orbit, and coordinate several intercepting transponders near each intended satellite, thereby requiring the expenditure of substantial resources to form complete interception coverage of a numerous-satellite system.
- Ensure that the interceptors' G/T are not much less than the G/T of the intended satellite uplink.

Even for an ideal system of this kind, there may be situations where the desired geolocation accuracy and processing speed are not readily available. For example, it would be difficult to distinguish multiple terminals that are simultaneously transmitting into a high-gain uplink beam using a low-data-rate mode near its threshold. In this case, numerous hops would be needed to find the peak of each terminal's ambiguity function, and much raw data would have to be stored before the various terminals could be differentiated.

## REFERENCES

1. S. Stein, "Algorithms for Ambiguity Function Processing," *IEEE Trans. Acoust., Speech, Signal Processing*, ASSP-29, 588-599 (1981).
2. P.C. Chestnut, "Emitter Location Accuracy Using TDOA and Differential Doppler," *IEEE Trans. Aerosp. Electron. Sys.*, AES-18, 214-218 (1982).
3. W.L. Stutzman and G.A. Thiele, *Antenna Theory and Design*, New York: Wiley (1981), Section 8.5.

# REPORT DOCUMENTATION PAGE

*Form Approved*  
**OMB No. 0704-0188**

Public reporting burden for this collection of information is estimated to average 1 hour per response, including the time for reviewing instructions, searching existing data sources, gathering and maintaining the data needed, and completing and reviewing the collection of information. Send comments regarding this burden estimate or any other aspect of this collection of information, including suggestions for reducing this burden, to Washington Headquarters Services, Directorate for Information Operations and Reports, 1215 Jefferson Davis Highway, Suite 1204, Arlington, VA 22202-4302, and to the Office of Management and Budget, Paperwork Reduction Project (0704-0188), Washington, DC 20503

1. AGENCY USE ONLY (Leave blank)	2. REPORT DATE 6 November 1990	3. REPORT TYPE AND DATES COVERED Technical Report	
4. TITLE AND SUBTITLE  Geolocation of Frequency-Hopping Transmitters via Satellite		5. FUNDING NUMBERS  C — F19628-90-C-0002 PE — 33110F, 33603F PR — 370	
6. AUTHOR(S)  Alexander Sonnenschein and Warren K. Hutchinson		8. PERFORMING ORGANIZATION REPORT NUMBER  TR-900	
7. PERFORMING ORGANIZATION NAME(S) AND ADDRESS(ES)  Lincoln Laboratory, MIT P.O. Box 73 Lexington, MA 02173-9108		10. SPONSORING/MONITORING AGENCY REPORT NUMBER  ESD-TR-90-115	
9. SPONSORING/MONITORING AGENCY NAME(S) AND ADDRESS(ES)  HQ AF Space Systems Division/MS Los Angeles AFB, CA 90009-2960		11. SUPPLEMENTARY NOTES  None	
12a. DISTRIBUTION/AVAILABILITY STATEMENT  Approved for public release; distribution is unlimited.		12b. DISTRIBUTION CODE	
13. ABSTRACT (Maximum 200 words)  <p style="text-align: center;">Satellite-communications terminal geolocation is analyzed by satellite interception, whereby a number of spaceborne interceptors transpond the frequency band of interest to a terrestrial location for processing. The general formulas for the interception accuracy are summarized, and a strawman interceptor system is proposed. Interception regions for prototypical terminals and satellites are calculated and the results are presented parametrically as a function of uplink SNR. The optimum angular separation of the interceptor satellites is found, and the effect of nonoptimal separation is discussed. The practical limitations involved in implementing this geolocation system are also discussed.</p>			
14. SUBJECT TERMS geolocation                      frequency-hopping                      ambiguity function satellite                            location finding		15. NUMBER OF PAGES 40	
		16. PRICE CODE	
17. SECURITY CLASSIFICATION OF REPORT Unclassified	18. SECURITY CLASSIFICATION OF THIS PAGE Unclassified	19. SECURITY CLASSIFICATION OF ABSTRACT Unclassified	20. LIMITATION OF ABSTRACT None